Impact of half-wave plate systematics on the measurement of cosmic birefringence from CMB polarization

Marta Monelli

Max Planck Institut für Astrophysik

Garching (Germany)

May 23th, 2023

CMB anisotropies

Inhomogeneities at photon decoupling imprint anisotropies on the CMB.

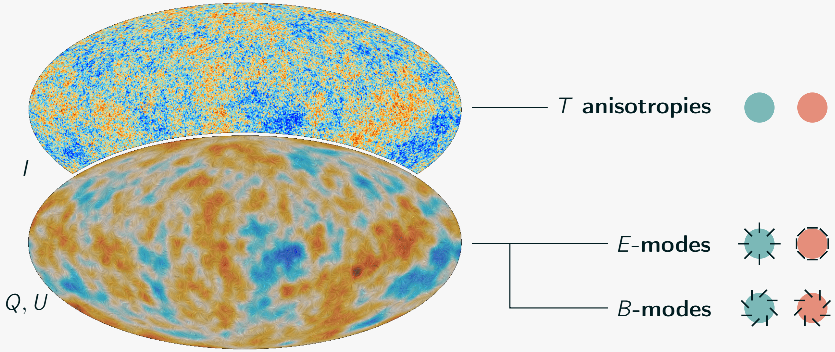

image credit: Jonathan Aumont

CMB anisotropies

Inhomogeneities at photon decoupling imprint anisotropies on the CMB.

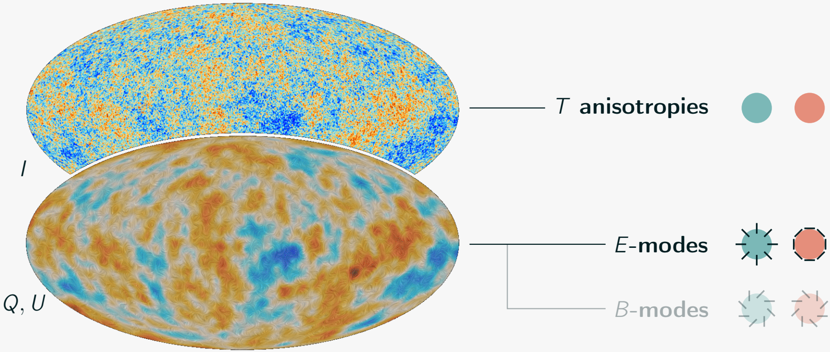

image credit: Jonathan Aumont

new physics from CMB polarization

- **Inflation**-sourced tensor perturbations are expected to leave a distinctive signature (B-modes) on CMB polarization.

This is driving the development of a number of new missions:

- ☐ Simons Observatory,
- ☐ South Pole Observatory,
- ☐ CMB Stage-4,
- ☐ **LiteBIRD**.

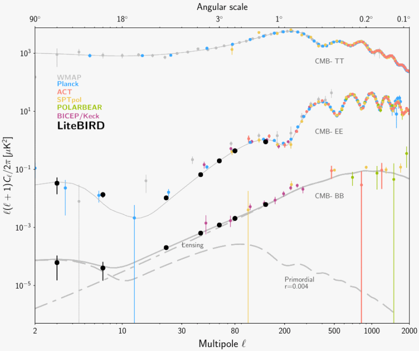

image credit: LiteBIRD Collaboration (2022) PTEP

new physics from CMB polarization

- **Inflation**-sourced tensor perturbations are expected to leave a distinctive signature (B-modes) on CMB polarization.

This is driving the development of a number of new missions:

- ☐ Simons Observatory,
- ☐ South Pole Observatory,
- ☐ CMB Stage-4,
- ☐ **LiteBIRD**.

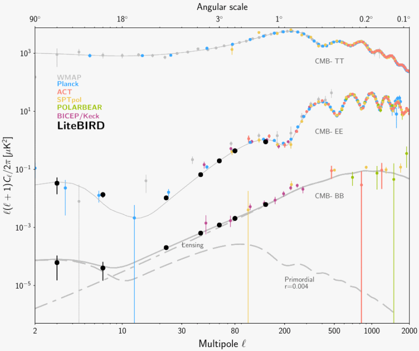

- **Parity-violating physics** could also imprint features on CMB polarization.

image credit: LiteBIRD Collaboration (2022) PTEP

signatures of parity violation

signatures of parity violation

Coupling a pseudoscalar χ to EM via a Chern-Simons term:

$$\mathcal{L}_{\mathsf{CS}} = -\frac{\alpha}{4f}\chi F_{\mu\nu}\widetilde{F}^{\mu\nu},$$

with $F_{\mu\nu} \propto \epsilon^{\mu\nu\rho\sigma} F_{\rho\sigma}$, makes $+$ and $-$ photon helicity states propagate differently:

$$A''_{\pm} + \left(k^2 \mp \frac{k\alpha\chi'}{f}\right) A'_{\pm} = 0.$$

Difference in phase velocity
$\rightarrow$ rotation of the plane of linear polarization.

signatures of parity violation

Coupling a pseudoscalar χ to EM via a Chern-Simons term:

$$\mathcal{L}_{\mathrm{CS}} = -\frac{\alpha}{4f}\chi F_{\mu\nu}\widetilde{F}^{\mu\nu},$$

with $F_{\mu\nu} \propto \epsilon^{\mu\nu\rho\sigma}F_{\rho\sigma}$, makes $+$ and $-$ photon helicity states propagate differently:

$$A''_{\pm} + \left(k^2 \mp \frac{k\alpha\chi'}{f}\right)A'_{\pm} = 0.$$

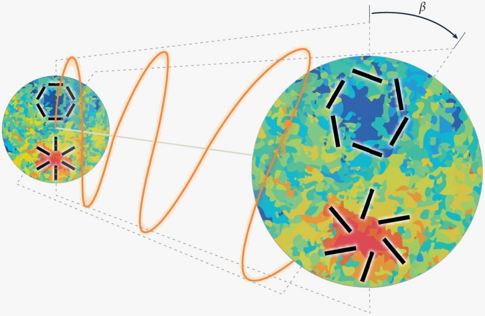

Difference in phase velocity
$\rightarrow$ rotation of the plane of linear polarization.

image credit: Yuto Minami

why “cosmic birefringence”?

Birefringence: property of a material whose refractive index depends on the polarization and propagation direction of light.

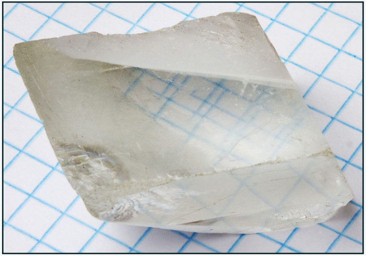

Thinner slabs, normal incidence: no double refraction, only retardance.

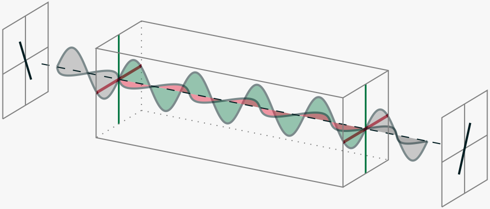

Both optical and cosmic birefringence rotate polarization vectors.

why “cosmic birefringence”?

Birefringence: property of a material whose refractive index depends on the polarization and propagation direction of light.

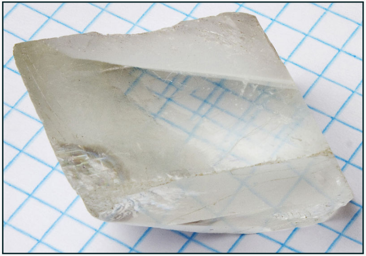

Thinner slabs, normal incidence:
no double refraction, only retardance.

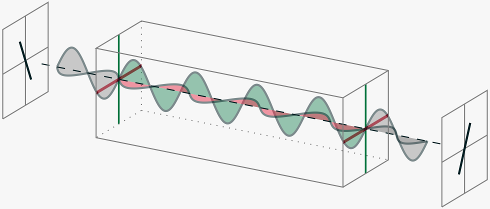

(this is a half-wave plate, by the way)

Both optical and cosmic birefringence rotate polarization vectors.

effect in harmonic space

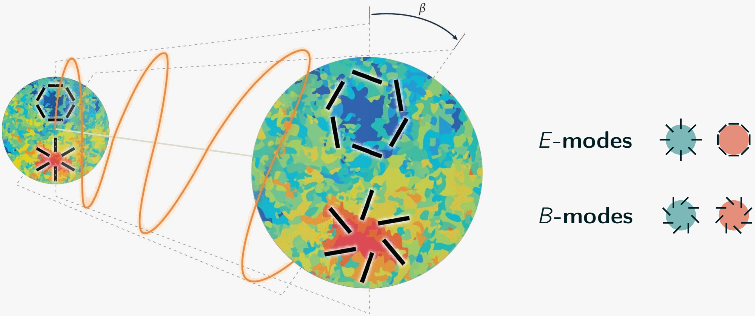

Mixing of E and B modes: $\begin{cases} a^E_{\ell m,\text{obs}} = a^E_{\ell m}\cos 2\beta - a^B_{\ell m}\sin 2\beta, \\ a^B_{\ell m,\text{obs}} = a^E_{\ell m}\sin 2\beta + a^B_{\ell m}\cos 2\beta. \end{cases}$

image credit: Yuto Minami

hints of cosmic birefringence

$$\begin{cases} C_{\ell,\mathrm{obs}}^{TT} = C_\ell^{TT}, \\ C_{\ell,\mathrm{obs}}^{EE} = \cos^2(2\beta) C_\ell^{EE} + \sin^2(2\beta) C_\ell^{BB} - \sin(4\beta) C_\ell^{EB}, \\ C_{\ell,\mathrm{obs}}^{BB} = \cos^2(2\beta) C_\ell^{BB} + \sin^2(2\beta) C_\ell^{EE} + \sin(4\beta) C_\ell^{EB}, \\ C_{\ell,\mathrm{obs}}^{TE} = \cos(2\beta) C_\ell^{TE} - \sin(2\beta) C_\ell^{TB}, \\ C_{\ell,\mathrm{obs}}^{EB} = \sin(4\beta)(C_\ell^{EE} - C_\ell^{BB})/2 + \cos(4\beta) C_\ell^{EB}, \\ C_{\ell,\mathrm{obs}}^{TB} = \sin(2\beta) C_\ell^{TE} + \cos(2\beta) C_\ell^{TB}. \end{cases}$$

$$\longrightarrow \quad C_{\ell,\mathrm{obs}}^{EB} = \tan(4\beta)(C_{\ell,\mathrm{obs}}^{EE} - C_{\ell,\mathrm{obs}}^{BB})/2.$$

hints of cosmic birefringence

$$
\begin{cases}
C_{\ell,\mathrm{obs}}^{TT} = C_\ell^{TT}, \\
C_{\ell,\mathrm{obs}}^{EE} = \cos^2(2\beta) C_\ell^{EE} + \sin^2(2\beta) C_\ell^{BB} - \sin(4\beta) C_\ell^{EB}, \\
C_{\ell,\mathrm{obs}}^{BB} = \cos^2(2\beta) C_\ell^{BB} + \sin^2(2\beta) C_\ell^{EE} + \sin(4\beta) C_\ell^{EB}, \\
C_{\ell,\mathrm{obs}}^{TE} = \cos(2\beta) C_\ell^{TE} - \sin(2\beta) C_\ell^{TB}, \\
C_{\ell,\mathrm{obs}}^{EB} = \sin(4\beta)(C_\ell^{EE} - C_\ell^{BB})/2 + \cos(4\beta) C_\ell^{EB}, \\
C_{\ell,\mathrm{obs}}^{TB} = \sin(2\beta) C_\ell^{TE} + \cos(2\beta) C_\ell^{TB}.
\end{cases}
$$

$$
\longrightarrow \quad C_{\ell,\mathrm{obs}}^{EB} = \tan(4\beta)(C_{\ell,\mathrm{obs}}^{EE} - C_{\ell,\mathrm{obs}}^{BB})/2.
$$

$$\beta = 0.35 \pm 0.14 \ (68\%\mathrm{CL})$$

To be confirmed (or not) by future polarization observations!

Minami and Komatsu (2020) Phys. Rev. Lett. 125

measuring polarization

describing polarization: Stokes vectors

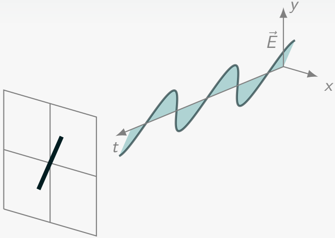

linearly polarized

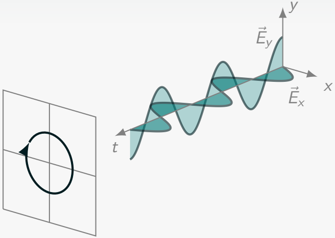

circularly polarized

$$\text{Stokes vector } \vec{S} \equiv \begin{pmatrix} I \\ Q \\ U \\ V \end{pmatrix} \equiv \begin{pmatrix} |E_x|^2 + |E_y|^2 \\ |E_x|^2 - |E_y|^2 \\ 2\mathrm{Re}(E_x E_y^*) \\ -2\mathrm{Im}(E_x E_y^*) \end{pmatrix}$$

describing polarization: Stokes vectors

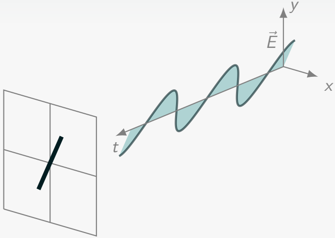

linearly polarized

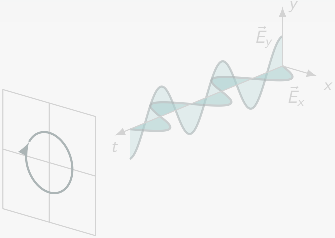

circularly polarized

$$\text{Stokes vector } \vec{S} \equiv \begin{pmatrix} I \\ Q \\ U \\ V \end{pmatrix} \equiv \begin{pmatrix} |E_x|^2 + |E_y|^2 \\ |E_x|^2 - |E_y|^2 \\ 2\mathrm{Re}(E_x E_y^*) \\ -2\mathrm{Im}(E_x E_y^*) \end{pmatrix}$$

describing polarization: Stokes vectors

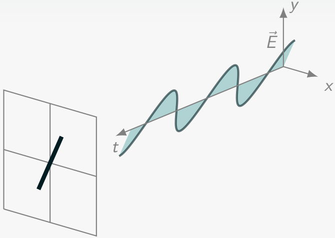

linearly polarized

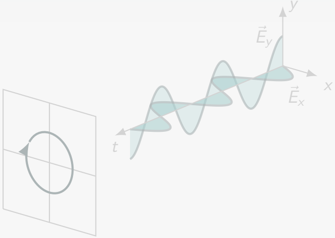

circularly polarized

$$\text{Stokes vector } \vec{S} \equiv \begin{pmatrix} I \\ Q \\ U \\ V \end{pmatrix} \equiv \begin{pmatrix} |E_x|^2 + |E_y|^2 \\ |E_x|^2 - |E_y|^2 \\ 2\mathrm{Re}(E_x E_y^*) \\ -2\mathrm{Im}(E_x E_y^*) \end{pmatrix}$$

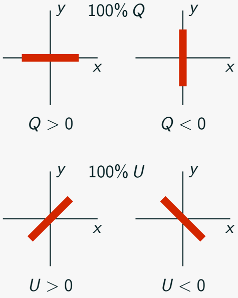

matrix methods for computing polarization

Mueller calculus: radiation described as $S = (I, Q, U)$, effect of polarization-altering devices parametrized by $\mathcal{M}$ so that $\mathsf{S}' = \mathcal{M} \cdot \mathsf{S}$.

$$\mathcal{M}_{\mathrm{pol}} = \frac{1}{2}\begin{pmatrix} 1 & 1 & 0 \\ 1 & 1 & 0 \\ 0 & 0 & 0 \end{pmatrix}, \quad \mathcal{M}_{\theta} = \begin{pmatrix} 1 & 0 & 0 \\ 0 & \cos(2\theta) & \sin(2\theta) \\ 0 & -\sin(2\theta) & \cos(2\theta) \end{pmatrix}, \quad \ldots$$

Given two optical elements in series with $\mathcal{M}_1$ and $\mathcal{M}_2$, their combined effect can be described by $\mathcal{M}_2\mathcal{M}_1$.

Matrix methods are extremely convenient to manipulate polarization, since one does not work with the electromagnetic field itself.

an example: pair-differencing systematics

Polarization can be measured by comparing the readings of pairs of (orthogonal) detectors:

$$
\begin{aligned}
d_1 &= a \cdot \mathcal{M}_{\mathrm{pol}} \cdot S = \begin{pmatrix} 1 & 0 & 0 \end{pmatrix} \frac{1}{2} \begin{pmatrix} 1 & 1 & 0 \\ 1 & 1 & 0 \\ 0 & 0 & 0 \end{pmatrix} \begin{pmatrix} I \\ Q \\ U \end{pmatrix} = I + Q \,, \\
d_2 &= a \cdot \mathcal{M}_{\mathrm{pol}} \mathcal{M}_{\pi/2} \cdot S = I - Q \,.
\end{aligned}
$$

This method can lead to detection of spurious polarization.

the path forward

How will next generation CMB experiments deal with this?

- LiteBIRD,
- Simons Observatory,
- South Pole Observatory,
- CMB Stage-4.

the path forward

How will next generation CMB experiments deal with this?

- ☑ LiteBIRD,
- ☑ Simons Observatory,
- ☑ South Pole Observatory,
- ☑ CMB Stage-4.

They **all** plan to employ rotating **half-wave plates (HWPs)** as polarization modulators.

the HWP: reducing systematics

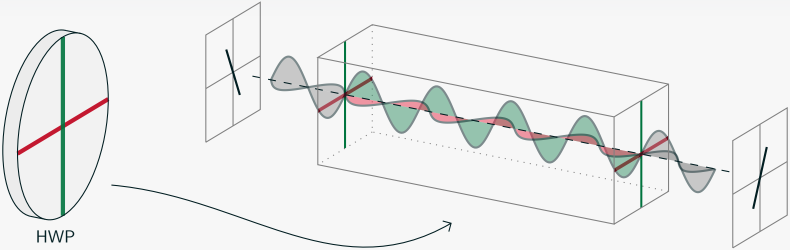

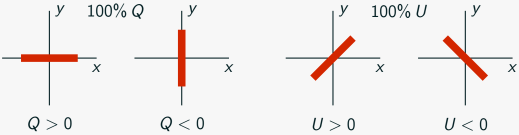

$$\mathcal{M}_{\text{HWP}} = \begin{pmatrix} 1 & 0 & 0 \\ 0 & 1 & 0 \\ 0 & 0 & -1 \end{pmatrix}$$

A **rotating** half-wave plate (HWP) as first optical element can help to control systematics.

ideal rotating HWP

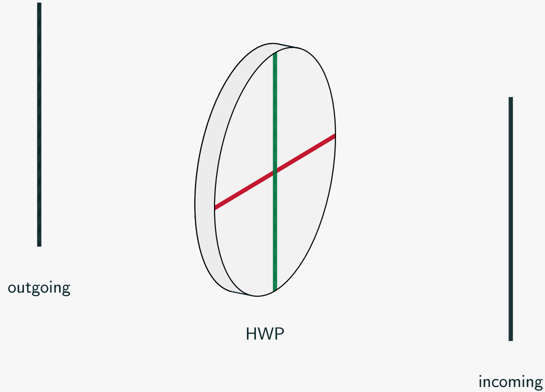

ideal rotating HWP

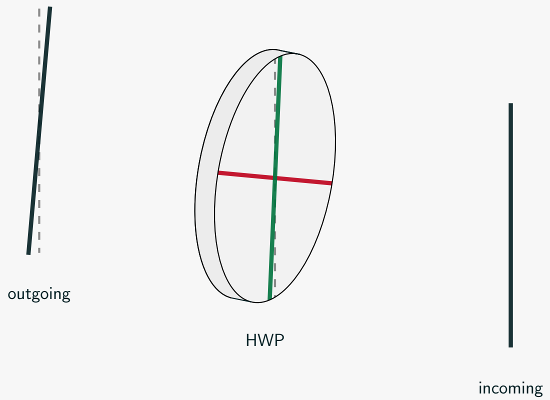

ideal rotating HWP

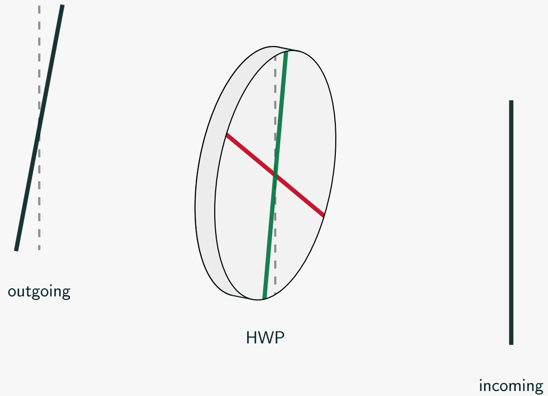

ideal rotating HWP

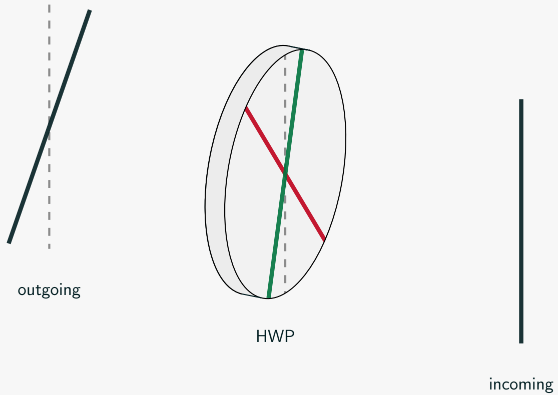

ideal rotating HWP

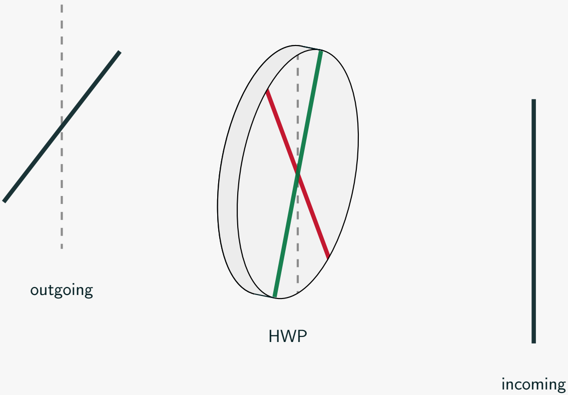

ideal rotating HWP

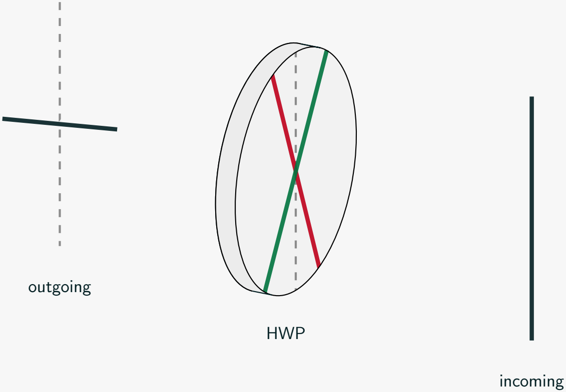

ideal rotating HWP

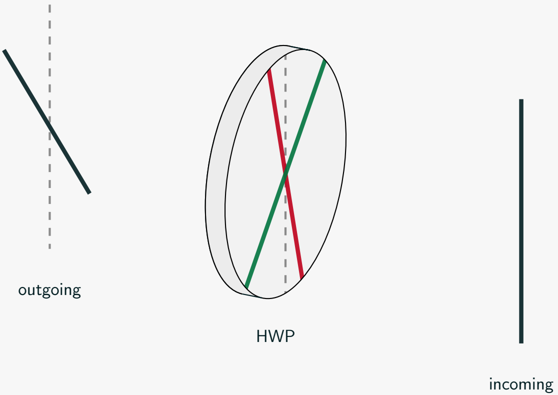

ideal rotating HWP

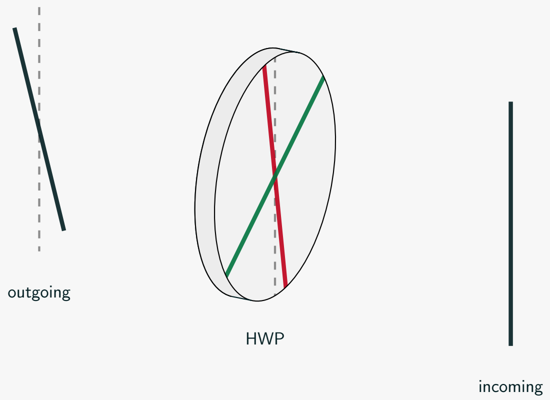

ideal rotating HWP

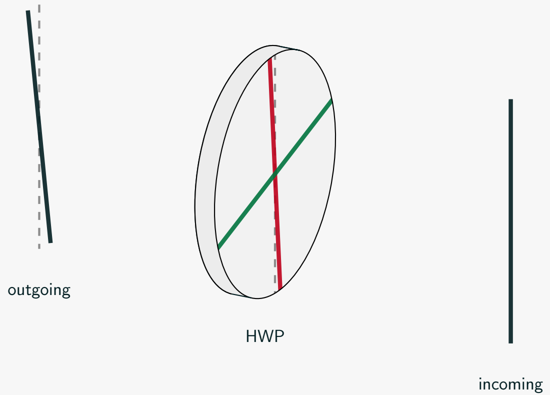

ideal rotating HWP

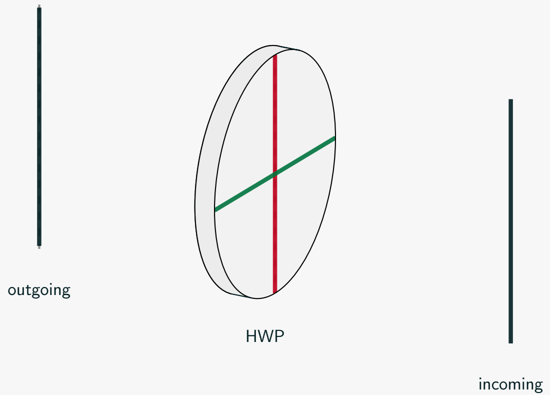

ideal rotating HWP

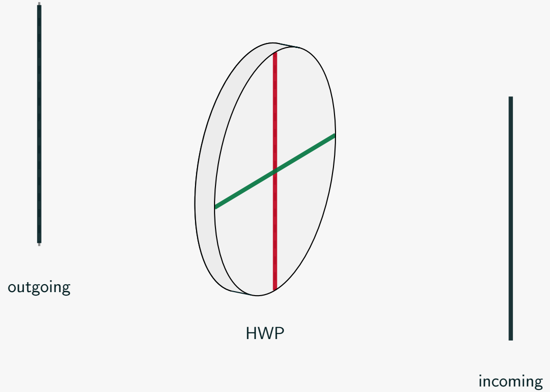

- The intrinsic signal is modulated to $4f_{\mathbf{HWP}}$ and can be distinguished from spurious signal (no/different modulation).

the HWP Mueller matrix

For an ideal HWP, $\mathcal{M}_{\text{ideal}} = \text{diag}(1, 1, -1, -1)$, but let's look at a realistic case:

$$\mathcal{M}_{\text{HWP}} = \left(\quad \right).$$

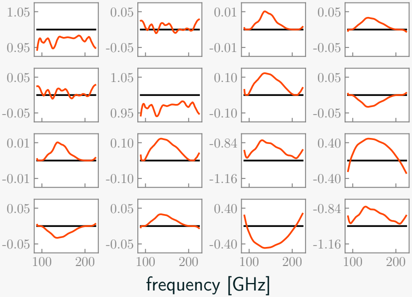

How does this affect the observed maps?

Giardiello et al. (2022) A&A 658

modeling the HWP effect

how to propagate systematics

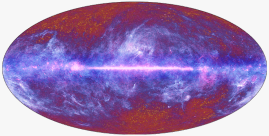

CMB sky maps

image credit: *Planck* collaboration

how to propagate systematics

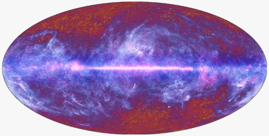

detection

time ordered data (TOD)

map-making

multi-frequency maps

foreground cleaning

CMB sky maps

TOD: collection of the signal detected by *each of the (4508) detectors* during *the whole (3-year) mission*.

image credit: *Planck* collaboration

how to propagate systematics

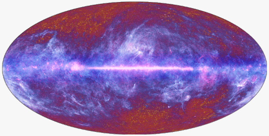

detection

time ordered data (TOD)

map-making

multi-frequency maps

foreground cleaning

CMB sky maps

TOD: collection of the signal detected by *each of the (4508) detectors* during *the whole (3-year) mission*.

Simulating and **modeling** TOD is crucial in the planning of any CMB experiment: it helps studying potential systematic effects.

image credit: *Planck* collaboration

HWP impact on CB: working assumptions

To focus on the impact of **HWP non-idealities** we consider a simplified problem:

- no noise,
- single frequency,
- CMB-only,
- simple beams,
- HWP aligned to the detector line of sight.

modeling the TOD

(minimal) TOD: signal detected by 4 detectors.

$$\begin{pmatrix} d^{(0)} \\ d^{(90)} \\ d^{(45)} \\ d^{(135)} \end{pmatrix} = \begin{pmatrix} (1\ 1\ 0) \cdot \mathcal{R}_{0-\phi} \mathcal{M}_{\mathrm{HWP}} \mathcal{R}_{\phi+\psi} \\ (1\ 1\ 0) \cdot \mathcal{R}_{90-\phi} \mathcal{M}_{\mathrm{HWP}} \mathcal{R}_{\phi+\psi} \\ (1\ 1\ 0) \cdot \mathcal{R}_{45-\phi} \mathcal{M}_{\mathrm{HWP}} \mathcal{R}_{\phi+\psi} \\ (1\ 1\ 0) \cdot \mathcal{R}_{135-\phi} \mathcal{M}_{\mathrm{HWP}} \mathcal{R}_{\phi+\psi} \end{pmatrix} \cdot \begin{pmatrix} I_{\mathrm{in}} \\ Q_{\mathrm{in}} \\ U_{\mathrm{in}} \end{pmatrix}$$

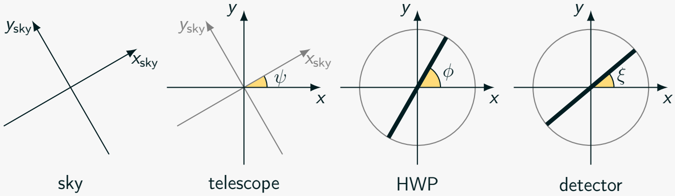

modeling the TOD

(minimal) TOD: signal detected by 4 detectors.

$$\begin{pmatrix} d^{(0)} \\ d^{(90)} \\ d^{(45)} \\ d^{(135)} \end{pmatrix} = \Big(\text{response matrix } A \Big) \cdot \begin{pmatrix} I_{\text{in}} \\ Q_{\text{in}} \\ U_{\text{in}} \end{pmatrix}$$

$$\begin{pmatrix} (1\ 1\ 0) \cdot \mathcal{R}_{0-\phi} \mathcal{M}_{\text{HWP}} \mathcal{R}_{\phi+\psi} \\ (1\ 1\ 0) \cdot \mathcal{R}_{90-\phi} \mathcal{M}_{\text{HWP}} \mathcal{R}_{\phi+\psi} \\ (1\ 1\ 0) \cdot \mathcal{R}_{45-\phi} \mathcal{M}_{\text{HWP}} \mathcal{R}_{\phi+\psi} \\ (1\ 1\ 0) \cdot \mathcal{R}_{135-\phi} \mathcal{M}_{\text{HWP}} \mathcal{R}_{\phi+\psi} \end{pmatrix}$$

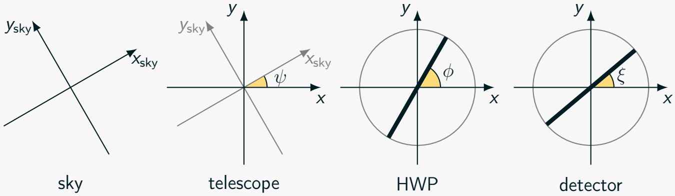

modeling the observed maps

map-maker: bin-averaging $\widehat{S} = (\widehat{A}^T \widehat{A})^{-1} \widehat{A}^T A \cdot S$ assuming ideal HWP.

$$\widehat{A} = \begin{pmatrix} (1\ 1\ 0) \cdot \mathcal{R}_{0-\phi} \mathcal{M}_{\text{ideal}} \mathcal{R}_{\phi+\psi} \\ (1\ 1\ 0) \cdot \mathcal{R}_{90-\phi} \mathcal{M}_{\text{ideal}} \mathcal{R}_{\phi+\psi} \\ (1\ 1\ 0) \cdot \mathcal{R}_{45-\phi} \mathcal{M}_{\text{ideal}} \mathcal{R}_{\phi+\psi} \\ (1\ 1\ 0) \cdot \mathcal{R}_{135-\phi} \mathcal{M}_{\text{ideal}} \mathcal{R}_{\phi+\psi} \end{pmatrix}$$

estimated ouput maps

$$\widehat{I} = m_{ii} I_{\rm in} + (m_{iq} Q_{\rm in} + m_{iu} U_{\rm in}) \cos(2\alpha) + (m_{iq} U_{\rm in} - m_{iu} Q_{\rm in}) \sin(2\alpha) \,,$$

$$\begin{aligned}
\widehat{Q} = \frac{1}{2}\Big\{&(m_{qq} - m_{uu}) Q_{\rm in} + (m_{qu} + m_{uq}) U_{\rm in} + 2 m_{qi} I_{\rm in} \cos(2\alpha) + 2 m_{ui} I_{\rm in} \sin(2\alpha) \\
&+ \big[(m_{qq} + m_{uu}) Q_{\rm in} + (m_{qu} - m_{uq}) U_{\rm in}\big] \cos(4\alpha) \\
&+ \big[-(m_{qu} - m_{uq}) Q_{\rm in} + (m_{qq} + m_{uu}) U_{\rm in}\big] \sin(4\alpha)\Big\} \,,
\end{aligned}$$

$$\begin{aligned}
\widehat{U} = \frac{1}{2}\Big\{&(m_{qq} - m_{uu}) U_{\rm in} - (m_{qu} + m_{uq}) Q_{\rm in} - 2 m_{ui} I_{\rm in} \cos(2\alpha) + 2 m_{qi} I_{\rm in} \sin(2\alpha) \\
&+ \big[-(m_{qq} + m_{uu}) U_{\rm in} + (m_{qu} - m_{uq}) Q_{\rm in}\big] \cos(4\alpha) \\
&+ \big[(m_{qu} - m_{uq}) U_{\rm in} + (m_{qq} + m_{uu}) Q_{\rm in}\big] \sin(4\alpha)\Big\} \,,
\end{aligned}$$

where $\alpha = \phi + \psi$. For **good** coverage and **rapidly spinning** HWP:

$$\widehat{\mathsf{S}} \simeq \begin{pmatrix} m_{ii} I_{\rm in} \\ [(m_{qq} - m_{uu}) Q_{\rm in} + (m_{qu} + m_{uq}) U_{\rm in}]/2 \\ [(m_{qq} - m_{uu}) U_{\rm in} - (m_{qu} + m_{uq}) Q_{\rm in}]/2 \end{pmatrix} .$$

Monelli et al. (2023) JCAP 03

angular power spectra

Expanding $\widehat{S}$ in spherical harmonics:

$$\widehat{C}_\ell^{TT} \simeq m_{ii}^2 C_{\ell,\mathrm{in}}^{TT},$$
$$\widehat{C}_\ell^{EE} \simeq \frac{(m_{qq}-m_{uu})^2}{4} C_{\ell,\mathrm{in}}^{EE} + \frac{(m_{qu}+m_{uq})^2}{4} C_{\ell,\mathrm{in}}^{BB} + \frac{(m_{qq}-m_{uu})(m_{qu}+m_{uq})}{2} C_{\ell,\mathrm{in}}^{EB},$$
$$\widehat{C}_\ell^{BB} \simeq \frac{(m_{qq}-m_{uu})^2}{4} C_{\ell,\mathrm{in}}^{BB} + \frac{(m_{qu}+m_{uq})^2}{4} C_{\ell,\mathrm{in}}^{EE} - \frac{(m_{qq}-m_{uu})(m_{qu}+m_{uq})}{2} C_{\ell,\mathrm{in}}^{EB},$$
$$\widehat{C}_\ell^{TE} \simeq \frac{m_{ii}(m_{qq}-m_{uu})}{2} C_{\ell,\mathrm{in}}^{TE} + \frac{m_{ii}(m_{qu}+m_{uq})}{2} C_{\ell,\mathrm{in}}^{TB},$$
$$\widehat{C}_\ell^{EB} \simeq \frac{(m_{qq}-m_{uu})^2-(m_{qu}+m_{uq})^2}{4} C_{\ell,\mathrm{in}}^{EB} - \frac{(m_{qq}-m_{uu})(m_{qu}+m_{uq})}{2} (C_{\ell,\mathrm{in}}^{EE} - C_{\ell,\mathrm{in}}^{BB}),$$
$$\widehat{C}_\ell^{TB} \simeq \frac{m_{ii}(m_{qq}-m_{uu})}{2} C_{\ell,\mathrm{in}}^{TB} - \frac{m_{ii}(m_{qu}+m_{uq})}{2} C_{\ell,\mathrm{in}}^{TE}.$$

Monelli et al. (2023) JCAP 03

analytical vs simulated output spectra

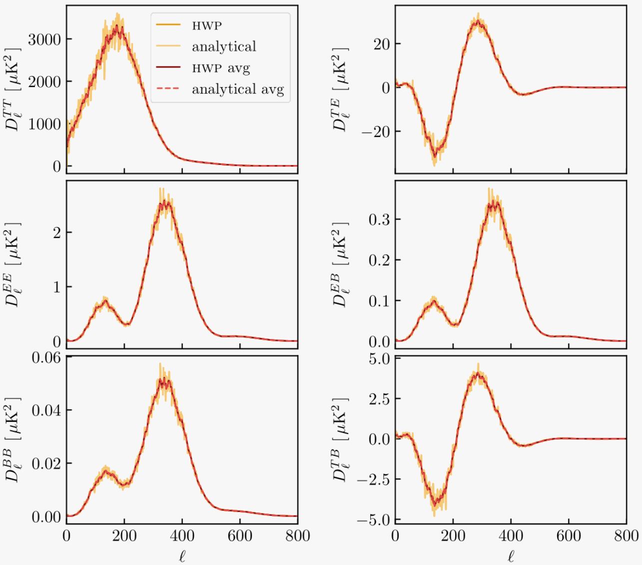

Monelli et al. (2023) JCAP 03

impact on cosmic birefringence

HWP-induced miscalibration

Analytic $\widehat{C}_\ell$s satisfy the relations:

$$\begin{cases} \widehat{C}_\ell^{EB} \simeq \tan(4\widehat{\theta}) \left[\widehat{C}_\ell^{EE} - \widehat{C}_\ell^{BB}\right]/2 \\ \widehat{C}_\ell^{TB} \simeq \tan(2\widehat{\theta})\widehat{C}_\ell^{TE} \end{cases}$$

The HWP induces an additional miscalibration, **degenerate** with cosmic birefringence and polarization angle miscalibration!

Monelli et al. (2023) JCAP 03

HWP-induced miscalibration

Analytic $\widehat{C}_\ell$s satisfy the relations:

$$\begin{cases} \widehat{C}_\ell^{EB} \simeq \tan(4\widehat{\theta}) \left[\widehat{C}_\ell^{EE} - \widehat{C}_\ell^{BB}\right]/2 \\ \widehat{C}_\ell^{TB} \simeq \tan(2\widehat{\theta})\,\widehat{C}_\ell^{TE} \end{cases}$$

our formulae suggest

$$\widehat{\theta} \equiv -\frac{1}{2}\arctan\frac{m_{qu}+m_{uq}}{m_{qq}-m_{uu}} \sim 3.8^\circ,$$

compatibly with simulations.

The HWP induces an additional miscalibration,
degenerate with cosmic birefringence and polarization angle miscalibration!

This doesn't mean that the HWP will keep us from measuring β, but it shows how important it is to carefully calibrate $\mathcal{M}_{\mathrm{HWP}}$.

Monelli et al. (2023) JCAP 03

conclusions and outlook

- much information is still hidden in CMB polarization (for instance, **cosmic birefringence** as a signature of parity-violating physics),
- new physics can be probed only if systematics are well under control,
- a rotating HWP can help, but it induces additional systematics which should be accounted for (**HWP-induced miscalibration**),

- we are now provided with an analytical model and a simulation pipeline that can be used to study the impact of the HWP in more realistic scenarios. this is key for the planning of the next generation of CMB experiments.